International Journal of Pharmaceutics 650 (2024) 123708

Contents lists available at ScienceDirect

International Journal of Pharmaceutics

journal homepage: www.elsevier.com/locate/ijpharm

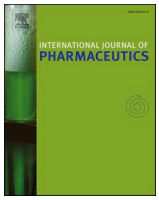

Coadministration of ABCB1/P-glycoprotein inhibitor elacridar improves tissue distribution of ritonavir-boosted oral cabazitaxel in mice

Nancy H.C. Loos [a], Margarida L.F. Martins [a], Daniëlle de Jong [b], Maria C. Lebre [a], Matthijs Tibben [b], Jos H. Beijnen [a,b,c], Alfred H. Schinkel [a,*]

[a] The Netherlands Cancer Institute, Division of Pharmacology, Amsterdam, The Netherlands
[b] The Netherlands Cancer Institute, Division of Pharmacy and Pharmacology, Amsterdam, The Netherlands
[c] Utrecht University, Faculty of Science, Department of Pharmaceutical Sciences, Division of Pharmacoepidemiology and Clinical Pharmacology, Utrecht, The Netherlands

ARTICLE INFO

Keywords:
Cabazitaxel/Jevtana
Ritonavir
Cytochrome P450 3A (CYP3A4)
Elacridar
P-glycoprotein (P-gp/ABCB1)
Pharmacokinetics

Compounds:
Cabazitaxel (PubChem CID 9854073)
Ritonavir (PubChem CID 392622)
Elacridar (PubChem CID 119373)

ABSTRACT

Developing an oral formulation for the chemotherapeutic cabazitaxel might improve its patient-friendliness, costs, and potentially exposure profile. Cabazitaxel oral availability is restricted by CYP3A-mediated first-pass metabolism, but can be substantially boosted with the CYP3A inhibitor ritonavir. We here tested whether adding the ABCB1/P-glycoprotein inhibitor elacridar to ritonavir-boosted oral cabazitaxel could further improve its tissue exposure using wild-type, CYP3A4-humanized and *Abcb1a/b*$^{-/-}$ mice. The plasma $AUC_{0\text{-}2h}$ of cabazitaxel was increased 2.3- and 1.9-fold in the ritonavir- and ritonavir-plus-elacridar groups of wild-type, and 10.5- and 8.8-fold in CYP3A4-humanized mice. Elacridar coadministration did not influence cabazitaxel plasma exposure. The brain-to-plasma ratio of cabazitaxel was not increased in the ritonavir group, 7.3-fold in the elacridar group and 13.4-fold in the combined booster group in wild-type mice. This was 0.4-, 4.6- and 3.6-fold in CYP3A4-humanized mice, illustrating that Abcb1 limited cabazitaxel brain exposure also during ritonavir boosting. Ritonavir itself was also a potent substrate for the Abcb1 efflux transporter, limiting its oral availability (3.3-fold) and brain penetration (10.6-fold). Both processes were fully reversed by elacridar. The tissue disposition of ritonavir-boosted oral cabazitaxel could thus be markedly enhanced by elacridar coadministration without affecting the plasma exposure. This approach should be verified in selected patient populations.

1. Introduction

Cabazitaxel is a semisynthetic taxane indicated for patients with castration-resistant prostate cancer, who showed progression during docetaxel treatment (Yared and Tkaczuk, 2012; FDA, 2010; EMA, 2011). Patients can develop resistance against docetaxel through different mechanisms, including expression of the cytochrome P450 enzyme 3A4 (CYP3A4) or of the multidrug efflux transporter P-glycoprotein (P-gp/ABCB1) at the tumor cell surface (Seruga et al., 2011; Ikezoe, 2004). Despite the limited molecular differences between cabazitaxel and docetaxel (2 methoxy instead of hydroxyl side groups; Figure S1), cabazitaxel exerts cytotoxicity in docetaxel-resistant tumor cells, which is possibly related to a higher tumor cell penetration (de Bono, 2010; Vrignaud, 2013). Additionally, cabazitaxel showed reduced transport by P-gp/ABCB1 compared to docetaxel (FDA, 2010; EMA, 2011).

Currently, cabazitaxel (25 mg/m^2 of body surface) is administered as a one-hour intravenous (i.v.) infusion every three weeks in combination with prednisolone (FDA, 2010; EMA, 2011). In contrast to oral therapy, which is relatively patient-friendly, this i.v. administration is time-consuming for patients with a hospital stay and they also have a high risk of developing injection site reactions (secondary side effects) (de Weger, 2021). The low aqueous solubility of taxanes necessitates the use of excipients in i.v. formulations that may cause hypersensitivity reactions. Therefore, our research group is interested in the development of oral formulations of taxanes, including cabazitaxel. However, the oral availability of taxanes is very low due to rapid metabolism by CYP3A4/5 in the liver and intestine and efflux by P-gp/ABCB1. This low oral availability of paclitaxel, docetaxel, and cabazitaxel could be significantly enhanced by coadministration of the CYP3A inhibitor ritonavir (Hendrikx, 2014; Hendrikx, 2013; van Waterschoot, 2009; Loos, 2023). Ritonavir (Fig. S2A) was initially developed as an HIV protease inhibitor, but is nowadays widely used as a booster drug in different treatment regimens due to its strong CYP3A inactivation capacity (Zhou, 2008; Macchiagodena et al., 2021; Hammond, 2022). Oral paclitaxel and

* Correspondence to: Division of Pharmacology, The Netherlands Cancer Institute, Plesmanlaan 121, 1066 CX Amsterdam, The Netherlands.
E-mail address: a.schinkel@nki.nl (A.H. Schinkel).

https://doi.org/10.1016/j.ijpharm.2023.123708
Received 9 October 2023; Received in revised form 11 December 2023; Accepted 12 December 2023
Available online 20 December 2023

docetaxel formulations in combination with ritonavir are currently tested in clinical studies (de Weger, 2021; Vermunt, 2021). Recently, we tested ritonavir as a booster of oral cabazitaxel in a transgenic CYP3A4 mouse strain, resulting in a ~ 34-fold increase in cabazitaxel plasma AUC compared to the vehicle-treated group (Loos, 2023).

In humans, cabazitaxel is metabolized by CYP3A4/5 for approximately 80–90 %, and to a lesser extent by CYP2C8. From the 20 metabolites formed *in vivo,* only three are pharmacodynamically active (FDA, 2010; EMA, 2011), two O-demethylated derivatives, DM1 and DM2, and docetaxel itself (Figure S1). Although they have a similar IC_{50} as cabazitaxel itself, none of them accounts individually for more than 10 % of the overall systemic exposure after intravenous administration in humans (EMA, 2011). The significant influence of CYP3A4 in liver and intestine on the oral availability and metabolite formation of cabazitaxel has been demonstrated in transgenic CYP3A mouse models (Tang, 2015). Interestingly, ritonavir showed non-linear pharmacokinetics and we previously demonstrated that also with lower doses of ritonavir significant increases in cabazitaxel plasma exposure in mice could be achieved (Loos, 2023).

The oral availability of paclitaxel and docetaxel is also restricted by the multidrug efflux transporter ABCB1 (Hendrikx, 2014; Hendrikx, 2013; van Waterschoot, 2009). P-gp/ABCB1 is an important member of the ATP-binding cassette (ABC) transporter family with broad substrate specificity (Schinkel and Jonker, 2003). These transporters are expressed at the apical side of cell membranes in various organs, such as the brain, liver, small intestine and kidney (Choudhuri and Klaassen, 2006). At the blood–brain-barrier (BBB), ABCB1 together with Breast Cancer Resistance Protein (BCRP/ABCG2) plays an essential role in protecting the brain by mediating efflux of their substrate drugs (Miller, 2014; Tang, 2013; Bao, 2020). Furthermore, the oral availability of ABC transporter substrates could be hampered by these transporters, because they mediate the efflux of their substrates from the bloodstream back into the intestinal lumen or from liver into the bile (Choudhuri and Klaassen, 2006; Szakács, 2008). A previous study showed that ABCB1 does not restrict the oral availability of cabazitaxel in mice. However, the brain accumulation was 10-fold reduced by murine Abcb1a/1b, but not Abcg2, and this could be completely reversed by coadministration of the dual ABCB1/ABCG2 inhibitor elacridar (structure in Fig. S2B) (Tang, 2015). Treatment with elacridar could be especially relevant to enhance the brain penetration, which might play an important role in the treatment of brain (micro-)metastases. Although brain metastases in prostate cancer patients are relatively rare, patients suffering from visceral metastases are more vulnerable to the development of brain metastasis (McBean et al., 2021; Bhambhvani, 2020; Myint and Qasrawi, 2021). Elacridar could further be beneficial to increase the intratumoral concentration of cabazitaxel when ABCB1 is upregulated at the tumor cell surface (Seruga et al., 2011). An increase in tissue distribution may result in more toxicity, which could be the case for cabazitaxel-ritonavir-elacridar treatment. However, if normal tissue is not affected, but only tumor tissue, this could be advantageous.

We here aimed to assess the combined impact of CYP3A and ABCB1 inhibition on the pharmacokinetics of oral cabazitaxel and its active metabolites in the context of ritonavir boosting, since the latter would usually apply in patients. We studied this by coadministration of elacridar and cabazitaxel with or without ritonavir in wild-type, CYP3A4-transgenic and Abcb1a/1b-deficient mouse models.

2. Materials and methods

2.1. Chemicals and reagents

The commercially available cabazitaxel formulation (Jevtana) was supplied by the hospital pharmacy of the Antoni van Leeuwenhoek hospital in Amsterdam, The Netherlands. Ritonavir was obtained from Sequoia Research Products (Pangbourne, United Kingdom). Elacridar HCl was purchased from Biosynth (Bratislava, Slovakia). Sodium chloride (0.9 %, w/v) was supplied by B. Braun Medical Supplies (Melsungen, Germany). Isoflurane was purchased from Virbac Nederland (Barneveld, The Netherlands), and heparin (5000 $IU{\cdot}mL^{-1}$) was obtained from Leo Pharma (Breda, The Netherlands). Bovine Serum Albumin (BSA) Fraction V was supplied by Roche Diagnostics GmbH (Mannheim, Germany). All other reagents and chemicals were purchased from Sigma-Aldrich (Steinheim, Germany).

2.2. Animals

Mice were housed and handled according to institutional guidelines in compliance with Dutch and EU legislation. All experimental animal protocols (under national permit numbers AVD301002016595 and AVD301002021147776) were approved by the institutional board for care and use of laboratory animals. As cabazitaxel is exclusively registered for the treatment of prostate cancer patients, experiments were performed in male wild-type, Cyp3aXAV (transgenic overexpression of human CYP3A4 in liver and intestine of *Cyp3a*$^{-/-}$), and *Abcb1a/1b*$^{-/-}$ mice. The animals were between 8 and 16 weeks of age and all mice had a > 99 % FVB genetic background. All experimental groups consisted of 6 mice. Mice were housed in a specific pathogen-free, temperature-controlled environment, including a controlled day-night cycle (12-hour light and 12-hour dark). The animals received a standard diet (Transbreed, SDS Diets, Technilab-BMI, Someren, The Netherlands) and acidified water *ad libitum*. Animal welfare was assessed before, during, and after the experiments.

2.3. Preparation of oral dosing solutions

All used drugs were orally administered by gavage using a blunt-ended needle. Cabazitaxel was used at a dose of 10 mg/kg of body weight. The Jevtana (10 mg/mL cabazitaxel) solution for infusion was diluted 10-fold with saline (NaCl 0.9 % w/v) to obtain the oral drug solution, yielding a concentration of 1 mg/mL. Jevtana contains 0.26 mg/mL polysorbate 80 and 15 % (w/v) ethanol and is adjusted to pH 2–6 with citric acid. Ritonavir was administered orally at a dose of 25 mg/kg of body weight and elacridar at a dose of 50 mg/kg of body weight. A stock solution of 12.5 mg/mL of ritonavir was prepared in polysorbate 80/ethanol (1:1, v/v) and this solution was diluted further (5-fold) with water to obtain a 2.5 mg/mL dosing solution. Elacridar hydrochloride was dissolved in DMSO (53 mg/mL), resulting in a stock solution of 50 mg elacridar base per mL. A mixture of polysorbate 80, ethanol and water (20:13:67, v/v/v) was added to the elacridar stock solution to obtain a 5 mg/mL oral dosing solution. For the combinational dosing of ritonavir and elacridar, a combined stock solution of 25 mg/mL ritonavir and 50 mg/mL elacridar was prepared in DMSO. This was then 10-fold diluted with a mixture of polysorbate 80, ethanol and water (20:13:67, v/v/v) to yield concentrations of 2.5 mg/mL ritonavir and 5 mg/mL elacridar in the oral dosing solution. The vehicle solution only contained polysorbate 80, ethanol and water (1:1:8, v/v/v). All oral dosing solutions were prepared freshly on the day of the experiment.

2.4. Pharmacokinetic study of cabazitaxel and metabolites in combination with ritonavir, elacridar or both

Prior to the experiments, mice were fasted for 3 to 4 h to reduce variance in oral absorption. After this fasting period, vehicle, ritonavir (25 mg/kg of body weight; 2.5 mg/mL dosing solution), elacridar (50 mg/kg of body weight; 5 mg/mL dosing solution) or ritonavir plus elacridar (25 mg/kg and 50 mg/kg of body weight; 2.5 mg/mL and 5 mg/mL dosing solution) were orally administered into the stomach of male wild-type, Cyp3aXAV, and *Abcb1a/1b*$^{-/-}$ mice using a blunt-ended needle. Subsequently, cabazitaxel (10 mg/kg of body weight; 1 mg/mL dosing solution) was orally administered by oral gavage 15 min after the vehicle or booster(s) administration. The 15-minute interval between the vehicle/booster and cabazitaxel administration was chosen based on

previous experiments showing that a sufficient level of mCyp3a and hCYP3A4 inhibition could be achieved within this timeframe (Loos, 2023). Tail vein blood collection (~50 μL per sample) using heparinized microvettes was performed at respectively 5, 10, 15, 30, and 60 min after the administration of cabazitaxel. The experiment was terminated at 2 h by performing cardiac puncture under isoflurane (3 %) anesthesia using a heparin-coated needle and syringe, followed by cervical dislocation of the anesthetized mice. Brain, liver, spleen, kidney, small intestine, and testis were collected. The small intestinal content (SIC) was collected by separation from the small intestinal tissue. The tissue was rinsed with saline to guarantee the removal of all feces. Tissues and matrices were homogenized in a FastPrep-24TM 5G homogenizer (M.P. Biomedicals, Santa Ana, CA) for 1 min with 1 mL 2 % (w/v) BSA in Milli-Q water added to brain, spleen and testis; 2 mL to kidney and SIC; and 3 mL to liver and small intestine. The plasma fraction was isolated from the blood samples using centrifugation at 9000*g* for 6 min at 4 °C. All samples were stored at −30 °C until analysis.

2.5. Bioanalytical assay

Bioanalysis of concentrations of cabazitaxel and its three active metabolites was performed using a specific, sensitive and validated liquid chromatography-tandem mass spectrometry (LC-MS/MS) method. With this method, the ritonavir concentrations were also measured within the same run, as previously described (Loos, 2023). The concentrations of cabazitaxel, docetaxel, and ritonavir were quantitatively determined, whereas DM1 and DM2 were semi-quantitatively determined in plasma samples and tissue homogenates by interpolation of the measured concentrations on the docetaxel calibration curve.

2.6. Pharmacokinetic calculations and statistical analysis

Non-compartmental analysis was used to estimate the pharmacokinetic parameters using the software package PK Solutions 2.0.2 (SUMMIT, Research Service). The plasma-concentration time curves and corresponding area under the curve (AUC) for all analyzed compounds were calculated using the linear trapezoidal rule without extrapolating to infinity. The peak plasma concentration (C_{max}) and the time to reach the maximum plasma concentration (T_{max}) were extrapolated directly from the raw data of each individual mouse. Statistical analysis and graph generation were performed using GraphPad Prism 9 (GraphPad Software Inc., La Jolla, CA). For multiple group comparisons, one-way analysis of variance (ANOVA) was calculated, and Sidak's *post hoc* correction was performed. In view of the often very large differences in means and standard deviations between groups, data were log-transformed before applying statistical analysis. Differences were considered statistically significant when $P < 0.05$. All data are presented as geometric mean ± SD.

3. Results

3.1. Oral availability of cabazitaxel is boosted by ritonavir, but not by elacridar

Previous *in vivo* studies showed that the oral availability of cabazitaxel is restricted by CYP3A and could be enhanced by coadministration of the CYP3A inhibitor ritonavir (Loos, 2023; Tang, 2015). Furthermore, intravenously administered elacridar (10 mg/kg) did not affect the plasma exposure of orally administered cabazitaxel and ABCB1/P-gp does not seem to play a role in the oral availability (Tang, 2015). In the clinical setting, it might at times be desirable to increase both the oral availability of cabazitaxel and enhance its relative brain distribution and/or tumor cell penetration, which could perhaps be achieved by coadministration of both oral ritonavir and elacridar. Therefore, the impact of combining these boosters on the oral pharmacokinetics of cabazitaxel was examined. We used male wild-type, Cyp3aXAV (*Cyp3a*$^{-/-}$ mice with transgenic overexpression of human CYP3A4 in liver and intestine) and *Abcb1a/1b*$^{-/-}$ mice. The Cyp3aXAV strain was included to assess the booster combination in the context of human CYP3A4 activity, and the *Abcb1a/1b*$^{-/-}$ strain to assess efficacy and specificity of the Abcb1 inhibition by elacridar and, in part, ritonavir. A (relatively short) 2-hour experiment was chosen to readily assess tissue distribution of cabazitaxel and its metabolites, as well as of ritonavir. Vehicle solution, ritonavir (25 mg/kg), elacridar (50 mg/kg) or ritonavir combined with elacridar were orally administered 15 min prior to the oral cabazitaxel (10 mg/kg) administration. The cabazitaxel plasma exposure was not significantly different between the wild-type and *Abcb1a/1b*$^{-/-}$ mice pretreated with vehicle solution, confirming that there was no impact of Abcb1a/b on its plasma pharmacokinetics (Fig. 1B and F). The CYP3A-mediated conversion of cabazitaxel was more extensive in the Cyp3aXAV transgenic mouse strain than in wild-type mice, based on the 5.8-fold lower $AUC_{0\text{-}2h}$ ($P < 0.0001$) and the 4.3-fold lower C_{max} ($P < 0.0001$) in the vehicle groups. Therefore, only direct comparisons between wild-type and *Abcb1a/1b*$^{-/-}$ mice are made and not between wild-type and Cyp3aXAV mice.

Coadministration of ritonavir resulted in a 2.3-fold ($P < 0.0001$) increase in cabazitaxel plasma $AUC_{0\text{-}2h}$ in wild-type and a 10.5-fold ($P < 0.0001$) enhancement in the Cyp3aXAV mice compared to their respective vehicle groups (Fig. 1A-D, Table S1). Ritonavir also increased the plasma $AUC_{0\text{-}2h}$ in *Abcb1a/1b*$^{-/-}$ mice by 1.7-fold ($P < 0.05$) (Fig. 1F, Table S1). In none of the analyzed mouse strains did elacridar coadministration influence the plasma exposure to cabazitaxel compared to their respective vehicle groups (Fig. 1, Table S1). Similar results for the plasma parameters ($AUC_{0\text{-}2h}$ and C_{max}) were further observed for the combined administration of ritonavir and elacridar compared to ritonavir alone, indicating that only ritonavir had a significant impact on the plasma exposure of cabazitaxel in all three strains (Fig. 1, Table S1).

3.2. Cooperative effect of ritonavir and elacridar on brain disposition of cabazitaxel

The influence of addition of both boosters on the tissue distribution of cabazitaxel was also studied. Due to their high Cyp3a/CYP3A4 content, liver and small intestine are the main organs for cabazitaxel metabolism. However, due to the large differences in overall plasma exposure (Fig. 1), absolute tissue concentrations will also differ extensively between the groups and strains. To correct for these differences, we primarily considered the tissue-to-plasma ratios. This showed that, with some notable exceptions, tissue concentrations primarily reflected the differences in plasma exposure between the groups within each strain (Fig. 2, Table S1).

The liver concentrations (Fig. 2A, Table S1) were highly increased in wild-type mice pretreated with ritonavir (4.6-fold, $P < 0.0001$) and with ritonavir and elacridar together (5.9-fold, $P < 0.0001$). Similar enhancements of the liver concentrations were observed in the *Abcb1a/1b*$^{-/-}$ mice pretreated with ritonavir (4.6-fold) or both boosters together (5.1-fold) (each $P < 0.0001$, Fig. 2A, Table S1). The impact of ritonavir on the liver concentrations was even more prominent in the Cyp3aXAV mice, with a 19.8-fold increase in the ritonavir group and a 26.3-fold increase in the double boosting group compared to their vehicle group (both $P < 0.0001$, Fig. 2A, Table S1). However, when considering the liver-to-plasma ratios, differences from the vehicle-only groups were much smaller (<2-fold) and mainly observed when at least ritonavir had been added (Fig. 2B, Table S1). Elacridar by itself had no significant impact. Collectively, these data suggest that liver disposition of cabazitaxel was primarily driven by its plasma levels, with a modest additional boost due to ritonavir.

Partly similar distribution patterns as for the liver were observed for the small intestinal tissue concentrations for all three mouse strains (Fig. 2C). However, considering the small intestine-to-plasma ratios, there was a significant 2- to 3-fold decrease in the ritonavir- and/or elacridar-treated groups in the wild-type and Cyp3aXAV mice, but not

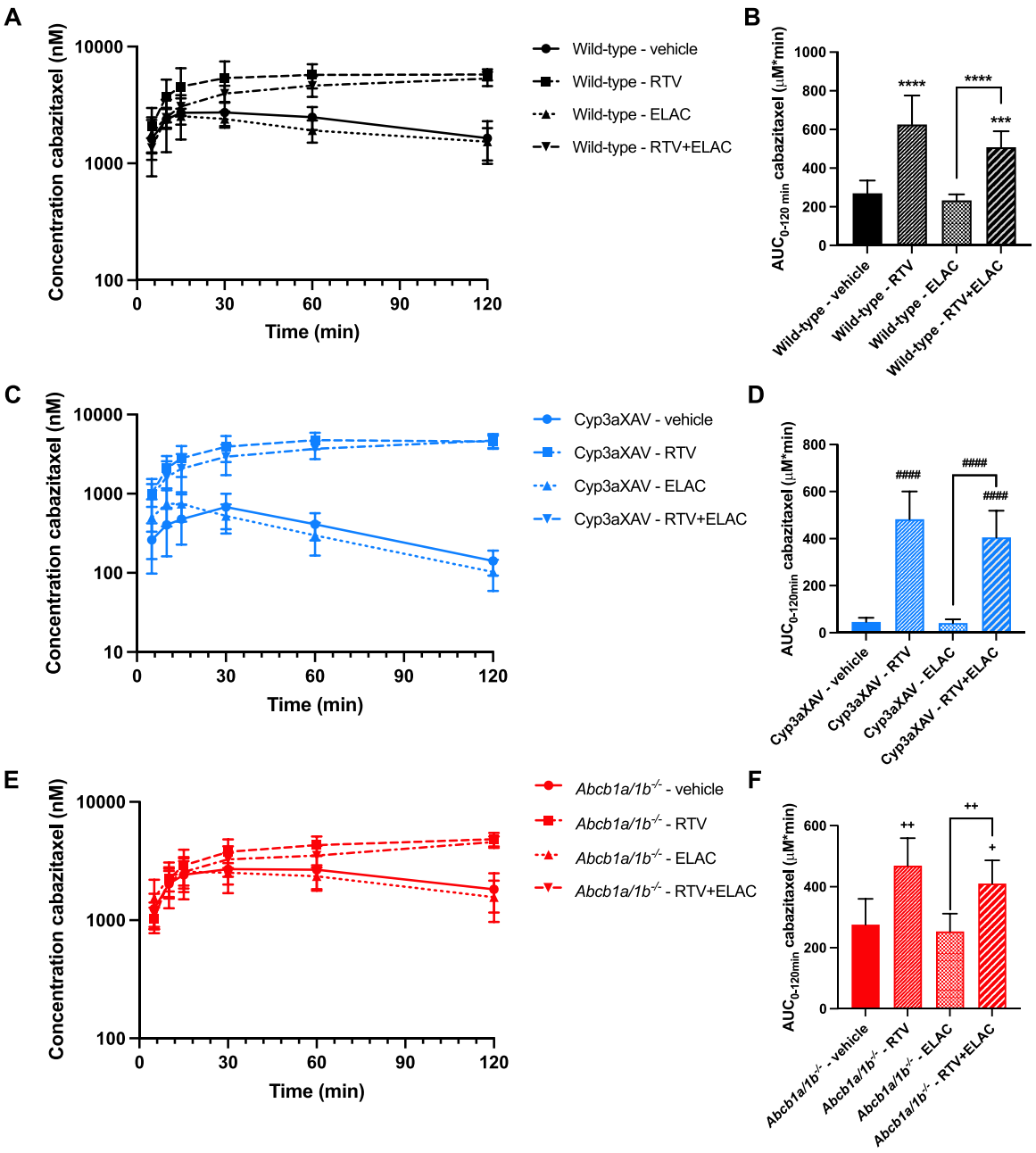

Fig. 1. Pharmacokinetic parameters of cabazitaxel in male wild-type, Cyp3aXAV and Abcb1a/1b$^{-/-}$ mice 2 h after oral administration of 10 mg/kg cabazitaxel in combination with vehicle, 25 mg/kg ritonavir, 50 mg/kg elacridar or both boosters combined (n = 6/group). **A.** Plasma concentration–time curve of cabazitaxel in wild-type mice. **B.** $AUC_{0\text{-}120min}$, area under the plasma concentration–time curve from 0 to 120 min in wild-type mice. **C.** Plasma concentration–time curve of cabazitaxel in Cyp3aXAV mice. **D.** $AUC_{0\text{-}120min}$ in Cyp3aXAV mice. **E.** Plasma concentration–time curve of cabazitaxel in Abcb1a/1b$^{-/-}$ mice. **F.** $AUC_{0\text{-}120min}$ in Abcb1a/1b$^{-/-}$ mice. Note the difference in Y-axis scales between the strains. Data are presented as mean ± SD. ***, $P < 0.001$; ****, $P < 0.0001$ compared to wild-type pretreated with vehicle or as indicated by the bar. $^{\#\#\#\#}$, $P < 0.0001$ compared to Cyp3aXAV pretreated with vehicle or as indicated by the bar. $^{+}$, $P < 0.05$; $^{++}$, $P < 0.01$ compared to Abcb1a/1b$^{-/-}$ pretreated with vehicle or as indicated by the bar.

the *Abcb1a/1b*$^{-/-}$ mice, compared to their respective vehicle groups (Fig. 2C and D). Of note, in the vehicle-treated *Abcb1a/1b*$^{-/-}$ mice, the tissue-to-plasma ratio was 2.5-fold lower compared to vehicle-treated WT and Cyp3aXAV mice, and neither ritonavir nor elacridar, nor its combination, further reduced these ratios. This suggests an involvement of Abcb1a/1b (inhibition) in the effects of ritonavir and elacridar on intestinal cabazitaxel distribution in the WT and Cyp3aXAV mice. This was further supported by the recovered percentage of dose in the small intestinal content (SIC), especially after correction for the plasma AUC (Fig. 2E and F). Coadministration of elacridar alone resulted in a 7.7-fold decrease in the recovered percentage of the cabazitaxel dose in SIC in wild-type and a 13.5-fold decrease in the transgenic Cyp3aXAV mice compared to their respective vehicle pretreated groups (Fig. 2E, Table S1). In contrast, elacridar or ritonavir alone or in combination had no significant effect on the percentage of dose recovered from *Abcb1a/1b*$^{-/-}$ SIC, even while this was markedly lower than in vehicle-treated wild-type SIC (Fig. 2E, Table S1). Correction for the plasma AUC confirmed that elacridar alone caused a marked reduction in the SIC-to-AUC ratios in wild-type and Cyp3aXAV mice, but not in *Abcb1a/1b*$^{-/-}$ mice (Fig. 2F). Given the specificity of the observed shifts, and that they were not observed in the *Abcb1a/1b*$^{-/-}$ mice, it is most likely that both elacridar and ritonavir substantially inhibited intestinal and possibly

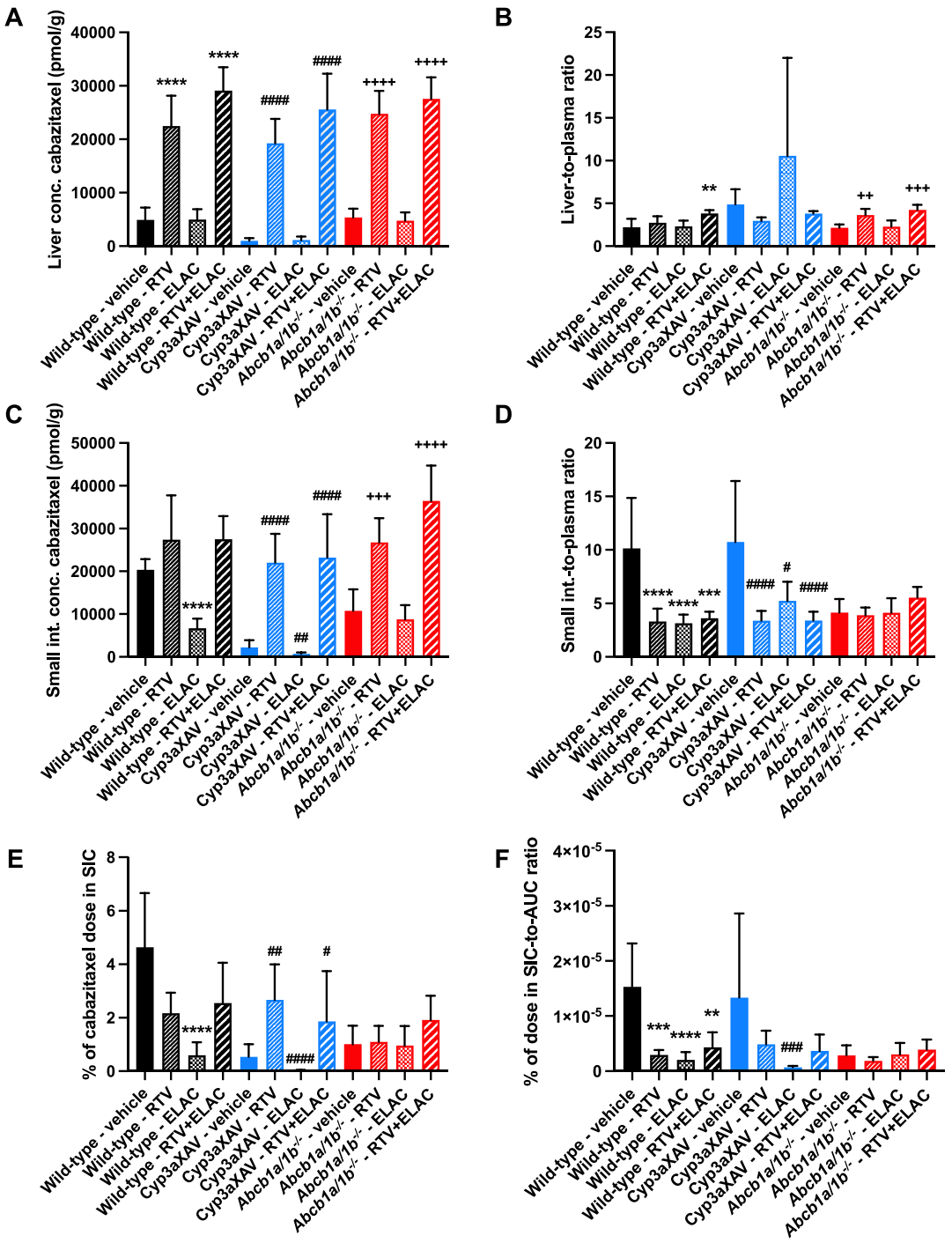

Fig. 2. Liver and small intestine exposure to cabazitaxel in male wild-type, Cyp3aXAV, and Abcb1a/1b$^{-/-}$ mice 2 h after oral administration of 10 mg/kg cabazitaxel in combination with vehicle, 25 mg/kg ritonavir, 50 mg/kg elacridar or both boosters combined (n = 6/group). **A.** Liver concentration. **B.** Liver-to-plasma ratio. **C.** Small intestine concentration. **D.** Small intestine-to-plasma ratio. **E.** Percentage of recovered cabazitaxel dose in small intestinal content (SIC). **F.** Percentage of recovered cabazitaxel dose in SIC-to-AUC ratio. Data are presented as mean ± SD. **, P < 0.01; ***, P < 0.001; ****, P < 0.0001 compared to wild-type pretreated with vehicle. $^{\#}$, P < 0.05; $^{\#\#}$, P < 0.01; $^{\#\#\#}$, P < 0.001; $^{\#\#\#\#}$, P < 0.0001 compared to Cyp3aXAV pretreated with vehicle. $^{+++}$, P < 0.001; $^{++++}$, P < 0.0001 compared to Abcb1a/1b$^{-/-}$ pretreated with vehicle.

hepatic Abcb1a/1b activity, resulting in more extensive intestinal absorption and/or reduced hepatobiliary excretion of cabazitaxel and thus relatively reduced SIC levels.

The absolute brain concentration and brain-to-plasma ratio of cabazitaxel were 9.5-fold and 8.3-fold higher, respectively, in vehicle-treated *Abcb1a/1b*$^{-/-}$ compared to wild-type mice, illustrating the strong impact of Abcb1a/1b on cabazitaxel brain penetration (Fig. 3A and B). As elacridar, given its high efficacy, can efficiently inhibit ABCB1 transporters at the BBB, we also studied the brain disposition of cabazitaxel in the different inhibitor-treated experimental groups (Fig. 3). The absolute brain concentration of cabazitaxel in wild-type mice was 3.7-fold increased in the ritonavir group, 6.2-fold in the elacridar group and 46-fold in the double-boosting group compared to the vehicle control group ($P < 0.0001$, Fig. 3A, Table S1). In the CYP3A4-transgenic mouse strain, the impact of ritonavir alone seems to be more prominent compared to elacridar alone (11.3- versus 3.2-fold increase) relative to

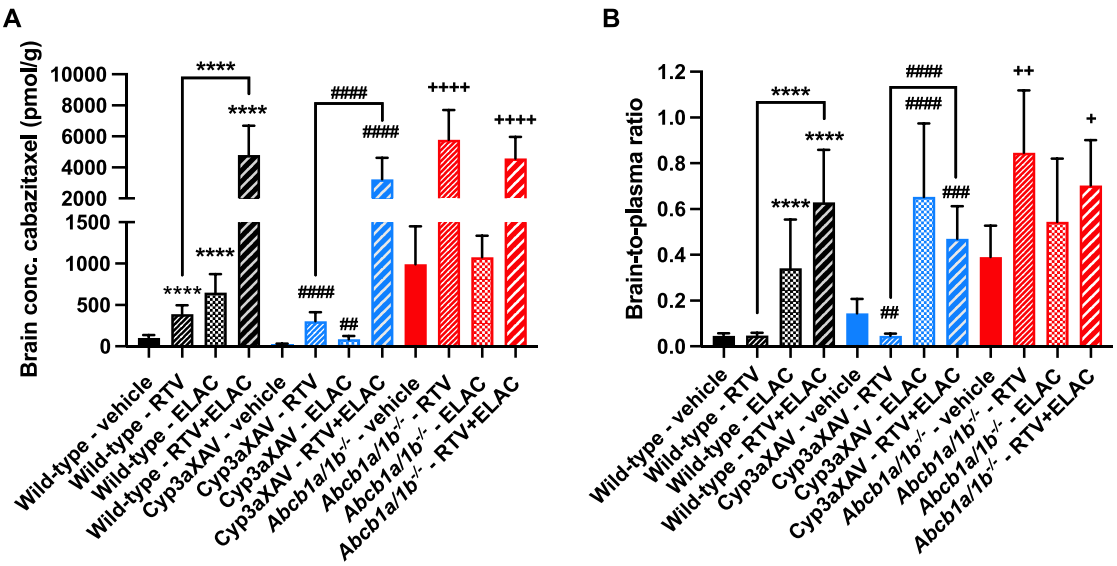

Fig. 3. Brain exposure to cabazitaxel in male wild-type, Cyp3aXAV, and Abcb1a/1b$^{-/-}$ mice 2 h after oral administration of 10 mg/kg cabazitaxel in combination with vehicle, 25 mg/kg ritonavir, 50 mg/kg elacridar or both boosters combined (n = 6/group). **A.** Brain concentration. **B.** Brain-to-plasma ratio at 2 h. Data are presented as mean ± SD. ****, P < 0.0001 compared to wild-type pretreated with vehicle or as indicated by the bar. $^{\#\#}$, P < 0.01; $^{\#\#\#}$, P < 0.001; $^{\#\#\#\#}$, P < 0.0001 compared to Cyp3aXAV pretreated with vehicle or as indicated by the bar. $^{+}$, P < 0.05; $^{++}$, P < 0.01; $^{++++}$, P < 0.0001 compared to Abcb1a/1b$^{-/-}$ pretreated with vehicle.

the vehicle-pretreated group (Fig. 3A, Table S1). However, combining the two boosters led to a 119-fold increase in absolute brain concentration ($P < 0.0001$, Fig. 3A, Table S1). These results indicate that ritonavir and elacridar together can play a strong cooperative role in enhancing the brain distribution of oral cabazitaxel. As expected, elacridar had no impact in the *Abcb1a/1b*$^{-/-}$ mice, but ritonavir still enhanced the absolute brain concentration in this mouse strain by 5.8-fold in the single-booster group and by 4.6-fold in the double-booster group ($P < 0.0001$, Fig. 3A), probably primarily through its effect on the cabazitaxel plasma exposure. The brain-to-plasma ratios confirmed the strong effect of elacridar on enhancing the relative brain penetration of cabazitaxel even in the presence of ritonavir, with 12.6-fold ($P < 0.0001$) and 9.4-fold ($P < 0.0001$) increases in the wild-type and Cyp3aXAV strains, respectively, when comparing double-boosted versus ritonavir only-treated mice, and no significant increase in the *Abcb1a/1b*$^{-/-}$ mice (Fig. 3B, Table S1). Therefore, both in the absence and presence of ritonavir, elacridar could markedly boost the relative brain penetration of cabazitaxel.

In spleen and kidney, no meaningful differences were observed, as the detected alterations appeared to be primarily driven by the differences in cabazitaxel plasma exposure between the different mouse strains and treatments (Fig. S3A-D). The relatively high tissue-to-plasma ratio values for spleen and kidney in the Cyp3aXAV mice for vehicle- and elacridar-treatments (Fig. S3B and D) are related to the unusually high impact of the transgenic CYP3A4 on the final cabazitaxel plasma concentration (Fig. 1). However, the testis-to-plasma ratios, similar to those in the brain, showed significant increases when comparing ritonavir plus elacridar-treated mice with ritonavir-only treated mice in the wild-type (5.8-fold, $P < 0.0001$) and Cyp3aXAV (5.1-fold, $P < 0.0001$), but not *Abcb1a/1b*$^{-/-}$ strains (Fig. S3F). This likely reflects inhibition of Abcb1a/1b activity by elacridar in the blood-testis barrier (BTB), even in the presence of ritonavir. While the tissue distribution was assessed at 2 h after cabazitaxel administration, as this was close to the cabazitaxel C_{max} for most of the mouse strains and conditions (Fig. 1), it is worth noting that the elacridar T_{max} is around 4 h after oral administration in mice (Ward and Azzarano, 2004). This means that the (essentially complete) level of Abcb1 inhibition we observed at 2 h will likely extend to at least 4 h, and probably considerably longer. Therefore, we conclude that we can achieve very extensive and prolonged inhibition of Abcb1 activity throughout the body using an oral elacridar and ritonavir coadministration regimen.

3.3. *Cabazitaxel active metabolite formation is strongly influenced by ritonavir, but not by elacridar*

The three active metabolites DM1, DM2 and docetaxel were also measured in plasma and tissues (Table S2). In vehicle-treated wild-type and *Abcb1a/1b*$^{-/-}$ mice, cabazitaxel reached the highest plasma exposure, followed by DM2 (Fig. 4). The plasma levels of DM1 and docetaxel were relatively low compared to those of cabazitaxel and DM2 (Fig. 4). In Cyp3aXAV mice, DM2 was the most abundant compound in plasma, suggesting high rates of formation of DM2 by the transgenic CYP3A4. These results are in agreement with previously published results on the highly CYP3A-dependent metabolism of cabazitaxel and its strong inhibition by ritonavir in the different strains (Loos, 2023; Tang, 2015).

As expected, ritonavir pretreatment in all the mouse strains led to a very marked inhibition of the metabolism of cabazitaxel, resulting in higher cabazitaxel plasma levels as previously seen in Fig. 1. The metabolites DM2 and docetaxel were not even detectable in wild-type and *Abcb1a/1b*$^{-/-}$ mice pretreated with ritonavir, whereas in the transgenic Cyp3aXAV mice still some formation was observed (Fig. 4). DM1 was still detectable, albeit at much reduced levels, perhaps indicating that its formation was less completely CYP3A-dependent compared to the other two metabolites (Fig. 4A and B). This is consistent with its known formation also in part by CYP2C8 in humans. These results indicate that all mCyp3a in the liver and intestine was likely fully inhibited during the 2 h after cabazitaxel was administered, in contrast to the likely more abundant hCYP3A4. The function of ritonavir-treated hCYP3A4 in the transgenic mouse strain appeared to be recovering over time given the gradual increase in DM2 and docetaxel formation (Fig. 4C and E), even while cabazitaxel plasma concentrations were plateauing (Fig. 1). This could be related to degradation by metabolism of ritonavir itself and/or gradual replacement of the inactivated CYP3A4 by newly formed enzyme(s). In the wild-type and *Abcb1a/1b*$^{-/-}$ mice pretreated with ritonavir, mCyp3a was apparently still non-functional at the time of termination. In contrast, in the vehicle-control groups of these mouse strains, metabolite formation started directly after cabazitaxel administration, as demonstrated before (Loos, 2023). Overall, given the limited effects observed in Fig. 4B, D, and F, it does not seem that elacridar coadministration in itself influences the metabolite formation

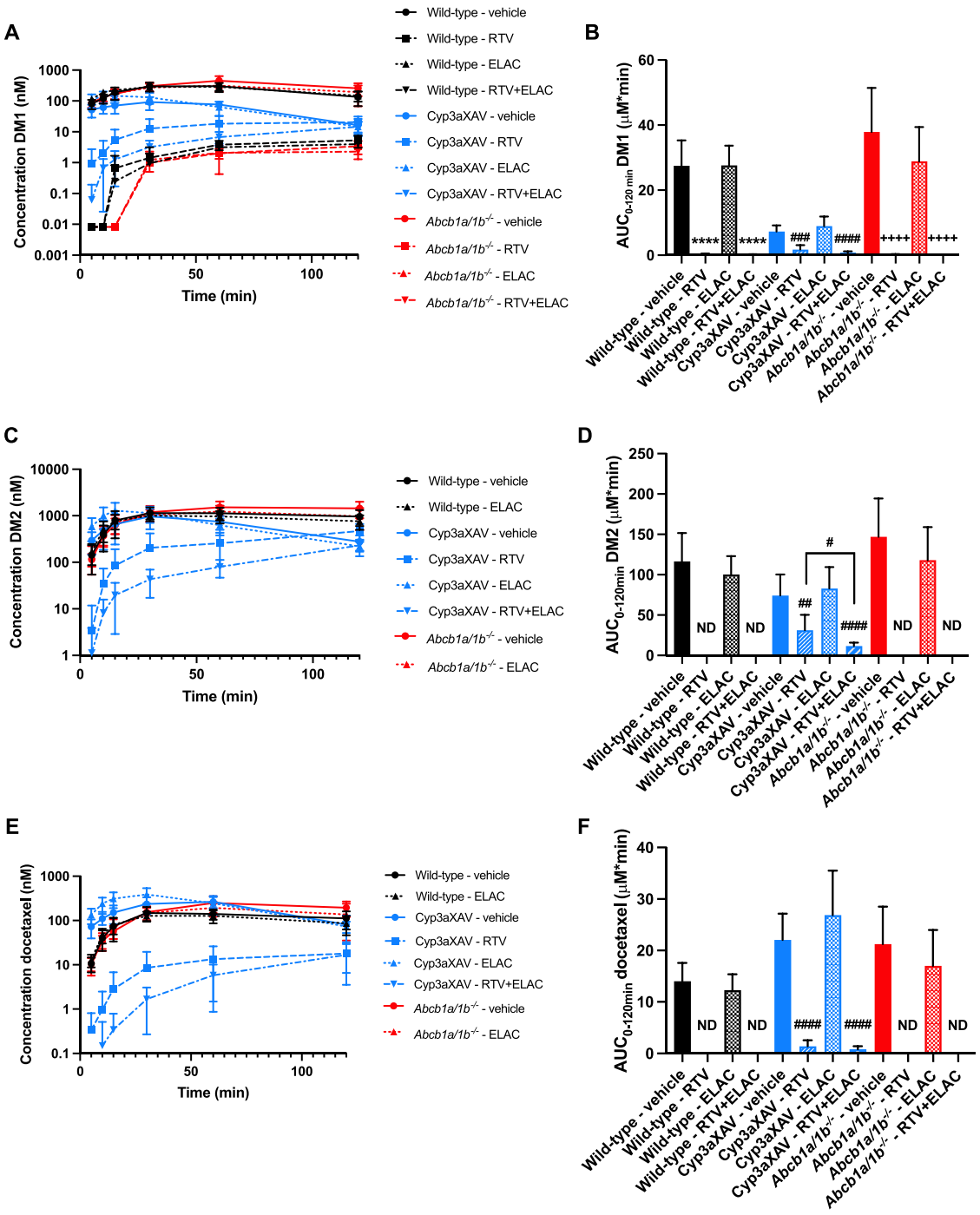

Fig. 4. Pharmacokinetic parameters of the three active metabolites of cabazitaxel (DM1, DM2, and docetaxel) in male wild-type, Cyp3aXAV, and Abcb1a/1b$^{-/-}$ mice 2 h after oral administration of 10 mg/kg cabazitaxel in combination with vehicle, 25 mg/kg ritonavir, 50 mg/kg elacridar or both boosters combined (n = 6/group). **A.** Plasma concentration–time curve of DM1. **B.** $AUC_{0\text{-}120min}$ of DM1. **C.** Plasma concentration–time curve of DM2. **D.** $AUC_{0\text{-}120min}$ of DM2. **E.** Plasma concentration–time curve of docetaxel. **F.** $AUC_{0\text{-}120min}$ of docetaxel. Data are presented as mean ± SD. ND, not datable; ****, $P < 0.0001$ compared to wild-type pretreated with vehicle. $^{\#\#}$, $P < 0.01$; $^{\#\#\#}$, $P < 0.001$; $^{\#\#\#\#}$, $P < 0.0001$ compared to Cyp3aXAV pretreated with vehicle or as indicated by the bar. $^{++++}$, $P < 0.0001$ compared to Abcb1a/1b$^{-/-}$ pretreated with vehicle.

markedly.

With respect to brain accumulation of the cabazitaxel metabolites, in all the ritonavir-treated wild-type and *Abcb1a/1b*$^{-/-}$ mice DM1, DM2, and docetaxel brain concentrations were undetectable or below the lower limit of quantification (LLoQ, Fig. 5). For these strains we therefore only present the data without ritonavir treatment. The brain-to-plasma ratio of DM1 in wild-type mice of the elacridar pretreated group was 2.4-fold increased ($P < 0.01$, Fig. 5B) compared to the vehicle group. The DM1 brain-to-plasma ratio of the vehicle group of the Abcb1-deficient mouse strain was even 4-fold higher compared to the wild-type vehicle group ($P < 0.0001$, Fig. 5B), and elacridar treatment did not significantly increase this further. This suggests that DM1 is a modest substrate for the Abcb1 transporter at the BBB. DM2 seems to be a more potent substrate for the Abcb1 transporter. The brain-to-plasma ratio of DM2 was 6.1-fold higher in both wild-type mice pretreated with elacridar and in the *Abcb1a/1b*$^{-/-}$ compared with wild-type mice pretreated

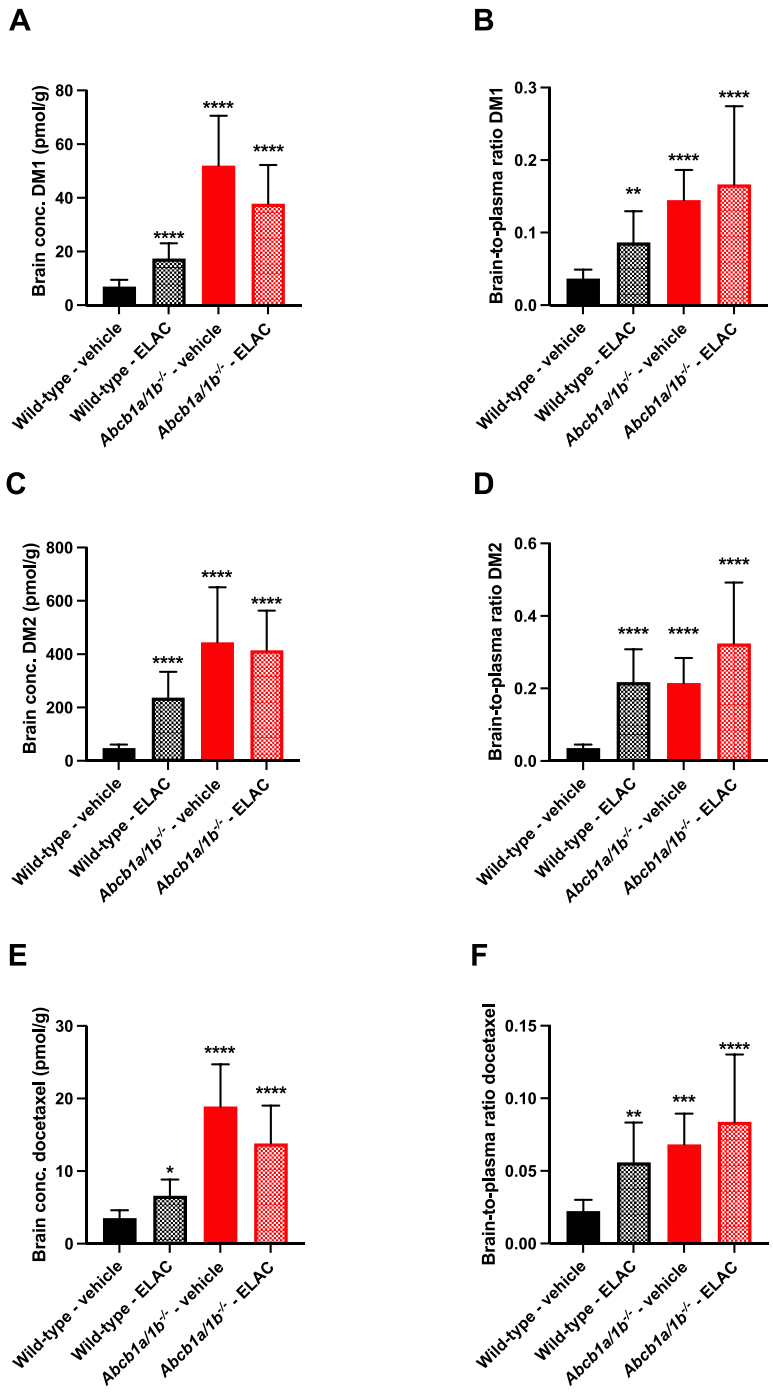

Fig. 5. Tissue distribution of the three active metabolites of cabazitaxel (DM1, DM2, and docetaxel) in male wild-type and Abcb1a/1b$^{-/-}$ mice 2 h after oral administration of 10 mg/kg cabazitaxel in combination with vehicle, 25 mg/kg ritonavir, 50 mg/kg elacridar or both boosters combined (n = 6/group). **A.** Brain concentration DM1. **B.** Brain-to-plasma ratio DM1. **C.** Brain concentration DM2. **D.** Brain-to-plasma ratio DM2. **E.** Brain concentration docetaxel. **F.** Brain-to-plasma ratio docetaxel. Data are presented as mean ± SD. *, P < 0.05; **, P < 0.01; ***, P < 0.001; ****, P < 0.0001 compared to wild-type pretreated with vehicle. The ritonavir and ritonavir-plus-elacridar pretreated groups have been omitted from the graphs, because the concentrations in these groups were below the Lower Limit of Quantification (LLoQ) or not even detectable.

with vehicle solution ($P < 0.0001$, Fig. 5D). The brain disposition for docetaxel seems to be similar to that of DM1 (Fig. 5E and F), indicating a modest role for Abcb1 in limiting the brain penetration of docetaxel.

The idea that DM1, DM2 and docetaxel are *in vivo* substrates for the Abcb1 transporter(s) is further supported by the excretion of these metabolites in the intestine. The recovered percentage of DM1 dose in SIC was 3.4-fold reduced in wild-type mice upon elacridar treatment ($P < 0.001$, Fig. S4A). A similar decrease was observed for the DM1 percentage of dose corrected for the plasma AUC (Fig. S4A and B). Similarly, for DM2 the SIC percentage of dose-to-AUC ratio was 9-fold ($P < 0.0001$, Fig. S4D) decreased in the wild-mice pretreated with elacridar compared to their vehicle group, whereas a reduction of 4.2-fold ($P < 0.01$, Fig. S4D) was observed in the vehicle-treated Abcb1-deficient mouse strain. Furthermore, Abcb1 might influence the intestinal excretion of docetaxel (Fig. S4E and F). The recovered percentage of dose as docetaxel in SIC corrected for the AUC was 3.8-fold ($P < 0.001$, Fig. S4F) lower in the elacridar-pretreated wild-type mice compared to the vehicle group, and in vehicle-treated *Abcb1a/1b*$^{-/-}$ mice it was

likewise decreased. Altogether, therefore, both elacridar treatment of wild-type mice and ablation of Abcb1a/1b resulted in markedly decreased recovery of all three cabazitaxel metabolites in the intestinal content, especially after correction for the plasma exposure. In contrast, elacridar treatment of *Abcb1a/1b*$^{-/-}$ mice did not cause significant changes in these parameters. Together, these data demonstrate the role of Abcb1a/1b in hepatobiliary and/or direct intestinal excretion of DM1, DM2, and docetaxel.

In the transgenic Cyp3aXAV strain, the impact of ritonavir and elacridar on metabolite formation was qualitatively similar to that in wild-type mice, except for the generally higher concentrations of metabolites in this strain. The tissue distribution in brain and the recovered percentages of dose in SIC are depicted in Figures S5 and S6, respectively. Qualitatively, the brain data were similar to what we observed in wild-type mice, with significant increases in brain-to-plasma ratios for DM2 upon elacridar treatment, but increases for DM1 and docetaxel were not significant. Similarly, in the additional presence of ritonavir, only DM2 showed a statistically significant increase in brain-to-plasma ratio due to elacridar treatment when directly comparing ritonavir-plus-elacridar *vs.* ritonavir-only groups (Fig. S5B, D and F). For the SIC, elacridar-only treatment caused a substantial decrease in recovered % of dose for DM1, DM2, and docetaxel (Fig. S6A, C and E), which was confirmed after correction for the plasma AUC (Fig. S6B, D and F). These results in Cyp3aXAV mice are in line with what we observed above in wild-type mice. In the additional presence of ritonavir such differences were less pronounced, in part also because of the much lower metabolite concentrations.

The differences in active metabolite concentrations in the other analyzed tissues of all three mouse strains appeared to be mainly driven by the differences in plasma exposure and are therefore not discussed here in detail (data not shown).

3.4. Pharmacokinetics of orally administered ritonavir

In a combined boosting situation, elacridar coadministration may also affect the pharmacokinetics of ritonavir, as this is itself a well-established transport substrate for Abcb1a/1b. However, the impact of its *in vivo* transportation by Abcb1 was not tested before in *Abcb1a/1b*-deficient mice. Therefore, the plasma concentrations and tissue distribution of ritonavir, which is also itself metabolized by CYP3A, were analyzed for the relevant cabazitaxel experimental mouse groups in the three mouse strains. As expected from previous studies, Cyp3aXAV mice showed a reduced ritonavir plasma AUC compared to wild-type mice, presumably because of extensive CYP3A4-mediated metabolism and binding of ritonavir (Fig. 6A and B). On the other hand, *Abcb1a/b*$^{-/-}$ mice showed an increased ritonavir plasma $AUC_{0\text{-}2h}$ (3.3-fold, $P < 0.01$) compared to wild-type mice, likely because Abcb1a/1b restricts the oral availability of ritonavir. The ritonavir $AUC_{0\text{-}2h}$ in the Cyp3aXAV was 3.0-fold lower ($P < 0.05$) compared to wild-type mice (Fig. 6B, Table S3). Similar results were observed for the C_{max} (Table S3). In accordance with the results in *Abcb1a/b*$^{-/-}$ mice, we observed modest but significant increases in the ritonavir C_{max} and $AUC_{0\text{-}120min}$ ($P < 0.05$) in the wild-type and CYP3A4 transgenic mice when treated with elacridar, but not in *Abcb1a/b*$^{-/-}$ mice (Fig. 6B, Table S3). These data indicate that ritonavir is a relatively potent *in vivo* substrate for Abcb1. It appears that Abcb1 is involved in the excretion of ritonavir and/or that ritonavir absorption is enhanced in the absence of Abcb1a/1b activity, resulting in higher plasma ritonavir exposure. It is worth noting that, although the oral formulations of the drugs contained significant amounts of polysorbate 80, which may inhibit Abcb1 activity to some extent, the pronounced effects of Abcb1 inhibition or ablation on ritonavir plasma levels (~3-fold increase, Fig. 6) indicate that there is still very substantial intestinal Abcb1 activity.

The brain-to-plasma ratio of wild-type mice was almost 11-fold ($P < 0.0001$) lower compared to that of the Abcb1-deficient mouse strain (Fig. 7B, Table S3), indicating a pronounced role for Abcb1 in limiting ritonavir brain exposure. Wild-type mice pretreated with the combination of ritonavir and elacridar demonstrated similarly high ritonavir brain distribution levels as the *Abcb1a/b*$^{-/-}$ mice (Fig. 7A and B). Elacridar treatment did not alter ritonavir relative brain distribution in *Abcb1a/b*$^{-/-}$ mice (Fig. 7B). These results indicate that the murine Abcb1-transporters at the BBB markedly restrict ritonavir brain penetration and can be fully and specifically inhibited by elacridar. In CYP3aXAV mice, despite the markedly lower absolute ritonavir concentrations in brain resulting from the lower plasma exposure (Figs. 6 and 7A), the relative brain distribution of ritonavir was similarly increased by elacridar treatment as in wild-type mice (Fig. 7B).

The recovered percentage of the ritonavir dose in the SIC was also significantly decreased by the absence of Abcb1a/1b or the coadministration of elacridar. In *Abcb1a/b*$^{-/-}$ mice, it was 8.5-fold ($P < 0.001$, Fig. 8A, Table S3) lower compared to that in wild-type mice. By inhibition of Abcb1a/1b by coadministration of elacridar, the percentage of dose in SIC was 3.6-fold ($P < 0.05$) reduced in the ritonavir and elacridar-treated wild-type group compared to the single ritonavir group (Fig. 8A, Table S3). The recovered percentage of dose in the ritonavir and elacridar-treated wild-type group was not significantly different

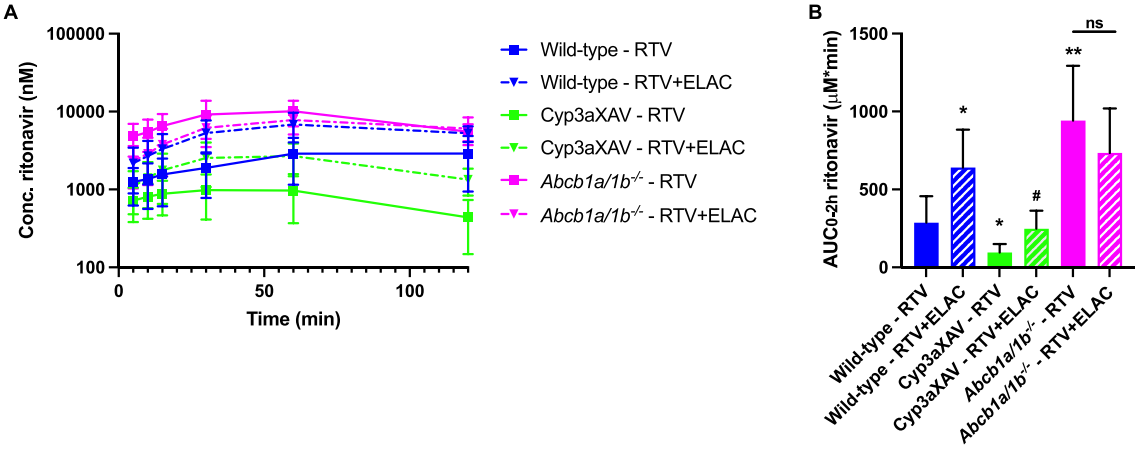

Fig. 6. Pharmacokinetic parameters of ritonavir in male wild-type, Cyp3aXAV (transgenic overexpression of human CYP3A4 in liver and intestine), and Abcb1a/1b$^{-/-}$ mice 2 h after oral administration of 10 mg/kg cabazitaxel in combination with 25 mg/kg ritonavir or ritonavir in combination with elacridar 50 mg/kg (n = 6/group). **A.** Plasma concentration–time curve of ritonavir (semi-log scale). **B.** $AUC_{0\text{-}120min}$, area under the plasma concentration–time curve from 0 to 120 min. Data are presented as mean ± SD. ns, not significant; *, P < 0.05; **, P < 0.01 compared to wild-type pretreated with ritonavir. #, P < 0.05 compared to Cyp3aXAV pretreated with ritonavir.

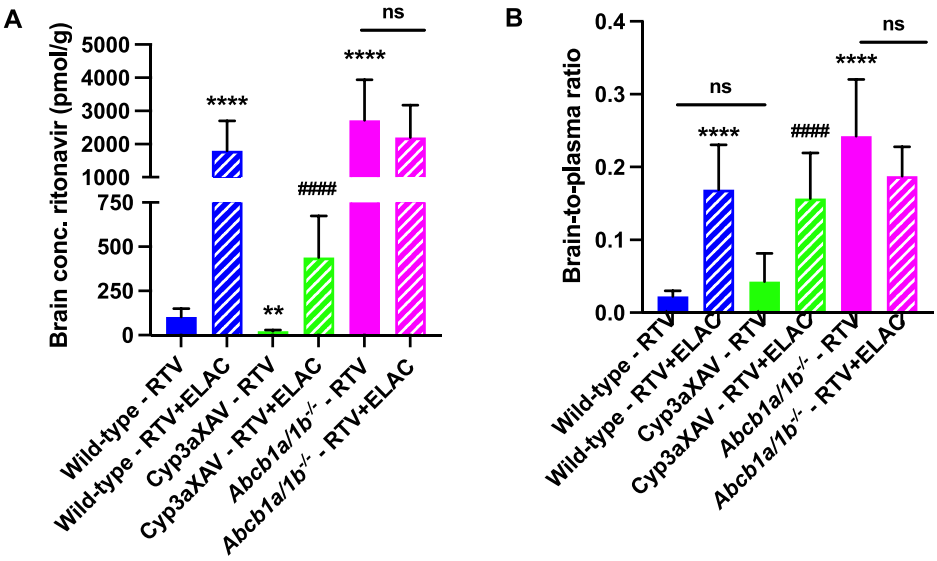

Fig. 7. Brain exposure to ritonavir in male wild-type, Cyp3aXAV, and Abcb1a/1b$^{-/-}$ mice 2 h after oral administration of 10 mg/kg cabazitaxel in combination with 25 mg/kg ritonavir or ritonavir in combination with elacridar 50 mg/kg (n = 6/group). **A.** Brain concentration. **B.** Brain-to-plasma ratio at 2 h. Data are presented as mean ± SD. ns, not significant; **, P < 0.01; ****, P < 0.0001 compared to wild-type mice pretreated with ritonavir. $^{\#\#\#\#}$, P < 0.0001 compared to Cyp3aXAV mice pretreated with ritonavir.

compared to both treatment groups of the *Abcb1a/b*$^{-/-}$ mice (Fig. 8A). This suggests involvement of Abcb1 in the hepatobiliary excretion of ritonavir and/or active transport of ritonavir by Abcb1 from the intestinal epithelium back to the intestinal lumen. In Cyp3aXAV mice, the addition of elacridar led to an 8.2-fold ($P < 0.001$) reduction in the SIC percentage of dose (Fig. 8A, Table S3). A very similar ritonavir distribution pattern was observed when the recovered percentages of dose were corrected for the plasma AUC (Fig. 8B). The % of dose-to-AUC ratio of ritonavir in wild-type mice was 11-fold ($P < 0.001$) reduced in the group with elacridar compared to the ritonavir group, whereas this was 21-fold in the CYP3A4 transgenic strain ($P < 0.0001$, Fig. 8B). These results clearly indicate a role for Abcb1 in the excretion (and/or reduced absorption) of ritonavir. There was no significant impact of the addition of elacridar in the *Abcb1a/b*$^{-/-}$ mice based on the ritonavir recovered percentage of dose (Fig. 8A and B), illustrating the relative specificity of the observed elacridar effects for Abcb1 inhibition in wild-type and Cyp3aXAV mice.

Abcb1 also appears to play an important role in limiting the testis distribution of ritonavir. The testis concentrations and tissue-to-plasma ratios were 15- and 7-fold (both $P < 0.0001$) higher, respectively, in the *Abcb1a/b*$^{-/-}$ mice compared to wild-type mice (Fig. 8C and D). Inhibition of Abcb1 by elacridar led to a significant increase in the testis concentrations and ratios (10.8- ($P < 0.0001$) and 8.0-fold ($P < 0.0001$), respectively) in the wild-mice (Fig. 8C and D). In Cyp3aXAV mice treated with ritonavir and elacridar the testis concentrations were significantly higher (5.4-fold, $P < 0.001$) compared to the ritonavir-pretreated group, and the same applied for the testis-to-plasma ratios (2.1-fold, $P < 0.01$, Fig. 8C and D). These shifts are very likely related to the elacridar-mediated Abcb1 inhibition, because there was no significant elacridar-induced difference in testis disposition of ritonavir in the *Abcb1a/b*$^{-/-}$ mice (Fig. 8C and D). For the other analyzed tissues, we did not observe meaningful differences apart from the expected lower ritonavir levels in Cyp3aXAV mice, albeit that the small intestinal tissue profile likely reflected in part the situation for the SIC (Figure S7).

4. Discussion

In this study, we found that the coadministration of oral ritonavir could significantly increase the oral availability and tissue disposition of orally administered cabazitaxel due to the potent inhibition of mCyp3a and hCYP3A4, consistent with previously obtained results (Loos, 2023). Furthermore, we demonstrated that under these ritonavir-boosted conditions, the coadministration of oral elacridar and/or the absence of active Abcb1a/1b could substantially enhance the distribution of cabazitaxel to some tissues without a significant influence on the oral availability. The plasma pharmacokinetics of cabazitaxel are therefore not affected by coadministration of elacridar and/or the absence of Abcb1a/1b activity, unlike its brain, testis, and small intestinal disposition. Although Abcb1 activity (and elacridar treatment) also affected the pharmacokinetics of the cabazitaxel metabolites, in the presence of ritonavir their relative formation was so strongly reduced that their pharmacodynamic impact relative to cabazitaxel is probably negligible. We further found that the pharmacokinetics of the booster ritonavir itself are also dramatically affected by Abcb1 activity, which limits the oral availability, brain and testis penetration, and intestinal disposition of ritonavir. Importantly, elacridar treatment also fully reversed all these Abcb1 functions with respect to ritonavir. We further did not observe any signs of short-term CNS-like toxicity in any of the combined boosting experiments, in contrast to the strong CNS-like toxicity we previously observed for some other drugs when Abcb1 activity was ablated or inhibited (Li, 2018; Li, 2021).

Boosting the tissue distribution of cabazitaxel with ritonavir in combination with elacridar could be beneficial for the treatment of patients with metastases in target organs protected by ABCB1 activity. Furthermore, upregulation of both CYP3A and/or ABCB1 in tumors could lead to tumor cell resistance against chemotherapy with substrate anticancer drugs, such as taxanes. The taxane treatment response could further be possibly affected by heterogeneous expression of CYP3A4, CYP3A5 and CYP2C8 in patients (van Eijk, 2019). Because the metabolism of cabazitaxel is mainly driven by CYP3A4 and to a lesser extent by CYP2C8, different expression levels of these enzymes could result in inter-individual differences in treatment response. Moreover, expression of ABCB1 was increased in prostate cancer cell lines, which are docetaxel-resistant compared to docetaxel-sensitive lines (Armstrong and Gao, 2015; Zhu, 2013). This results in enhanced drug efflux and eventually drug resistance to docetaxel. This acquired drug resistance could lead to switching prostate cancer patients from docetaxel to cabazitaxel, which is considered to be less subject to ABCB1-mediated drug

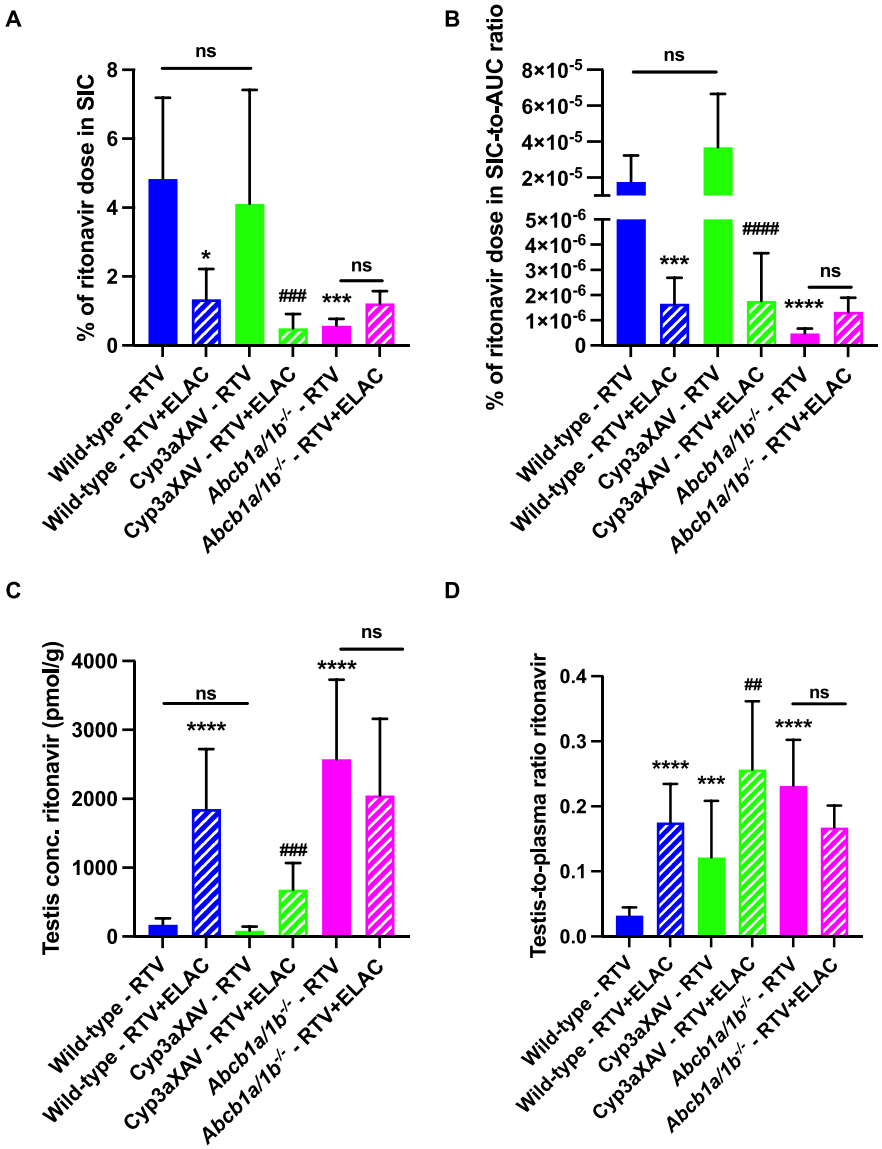

Fig. 8. Tissue exposure to ritonavir in male wild-type, Cyp3aXAV and Abcb1a/1b$^{-/-}$ mice 2 h after oral administration of 10 mg/kg cabazitaxel in combination with 25 mg/kg ritonavir or ritonavir in combination with elacridar 50 mg/kg (n = 6/group). **A.** Percentage of recovered ritonavir dose in small intestinal content (SIC). **B.** Percentage of recovered ritonavir dose in SIC-to-AUC ratio. **C.** Testis concentration. **D.** Testis-to-plasma ratio. Data are presented as mean ± SD. ns, not significant; *, $P < 0.05$; ***, $P < 0.001$; ****, $P < 0.0001$ compared to wild-type pretreated with ritonavir. $^{\#\#}$, $P < 0.01$; $^{\#\#\#}$, $P < 0.001$; $^{\#\#\#\#}$, $P < 0.0001$ compared to Cyp3aXAV pretreated with ritonavir.

resistance. However, our data still show a marked impact of Abcb1 on the *in vivo* efflux of cabazitaxel and its metabolites, limiting cabazitaxel brain and testis penetration in mice. These results indicate that cabazitaxel is still very effectively transported by Abcb1 across the BBB. Addition of elacridar could reverse the effects of Abcb1 and therefore possibly overcome drug resistance or tissue protection due to ABCB1 (over-)expression, although brain metastases are relatively rare in prostate cancer patients (McBean et al., 2021; Bhambhvani, 2020; Myint and Qasrawi, 2021). However, there appears to be a relationship between the occurrence of visceral metastases in prostate cancer and a higher incidence of brain metastasis (Myint and Qasrawi, 2021). Nonetheless, a previously performed Phase I study with docetaxel and zosuquidar, another ABCB1 inhibitor, showed only minimal alterations in docetaxel pharmacokinetics and clinical activity (Fracasso, 2004). Coadministration of ritonavir resulted in enhanced tissue distribution of cabazitaxel due to increased systemic levels, as previously shown by us (Loos, 2023), but the addition of elacridar could increase the relative extent of tissue penetration even further. Our data show that there is a strong cooperative effect of combining both boosters (ritonavir and elacridar), especially for the brain disposition of cabazitaxel. Therefore, coadministration of ritonavir and elacridar together could possibly also result in an increased penetration in tumor cells (over-)expressing ABCB1, and, where relevant, tumors positioned behind a functional blood–brain barrier. This could lead to a better outcome for patients treated with oral cabazitaxel. It is worth mentioning, though, that elacridar has a much better oral (and linear) availability in mice than in humans. It may therefore require further optimization of the formulation of this otherwise well-tolerated inhibitor to achieve suitable availability in humans as well (Ward and Azzarano, 2004; Kuppens, 2007). It is further worth mentioning that early clinical trials that failed to show clear benefits of coadministering ABCB1 inhibitors during chemotherapy of possible multidrug-resistant cancer may, retrospectively, have been designed suboptimally (Robey, 2018). This could be improved by for instance being more selective in the properties of tumors being included in such studies. Also, additional toxicity was seen in inhibitor trials due to unforeseen increased systemic exposure of the

chemotherapeutics. However, in the context of trials to improve oral availability of taxanes such as cabazitaxel using the CYP3A inhibitor ritonavir, systemic levels of the drug would obviously be monitored carefully, and doses could be adjusted accordingly. In addition, the possible occurrence of any qualitative shifts in toxicity should first be critically monitored and evaluated in small trials in patients.

CYP3A4 is most abundant in the liver and small intestine. Therefore, these organs are important to study when applying CYP3A inhibitors, such as ritonavir. Our results showed that the liver disposition of cabazitaxel is clearly increased by ritonavir, but this was mainly driven by the higher plasma exposure in these treatment groups. There was no obvious influence of elacridar on the liver distribution of cabazitaxel (Fig. 2A and B). This is in contrast to the small intestinal disposition, where we did observe an impact of the Abcb1 transporter and its inhibition by elacridar. Ritonavir is not only an irreversible inhibitor of CYP3A, but it also has some Abcb1 inhibition capacity (Kharasch, 2008). The ABCB1 inhibitory potency of ritonavir seems to be more prominent in the liver and intestine compared to the BBB (Kharasch, 2008; Holmstock, 2010; Bachmeier, 2005). This is consistent with the results of our study and likely has to do with the much higher local concentrations of ritonavir in liver and intestine compared to brain. Ritonavir drastically enhanced the plasma pharmacokinetics of cabazitaxel, but not the brain-to-plasma ratios in the wild-type and Cyp3aXAV mice. In intestinal tissue, most likely both ritonavir and elacridar substantially inhibited the intestinal Abcb1, resulting in a reduced hepatobiliary excretion and/or more extensive net absorption in the intestinal lumen of cabazitaxel in wild-type mice (Fig. 2E and F). Furthermore, we observed a potent inhibition of the Abcb1 activity in the blood-testis-barrier by elacridar, even in the presence of ritonavir (Fig. S3E and F). This suggests that also at the BTB local ritonavir concentration is not high enough to substantially inhibit Abcb1 activity.

There is a high hepatic and intestinal expression of CYP3A4 in the Cyp3aXAV mice, resulting in a relatively more rapid biotransformation of ritonavir and, subsequently, cabazitaxel in this mouse strain compared to wild-type mice. CYP3A will remain non-functional after inhibition by ritonavir due to the primarily irreversible nature of this inactivation (Zhou, 2008; Rock, 2014). The inactivated CYP3A needs to be replaced by newly synthesized enzymes, which in humans should take around three days based on the enterocyte turnover rate (Darwich, 2014). For mouse Cyp3a, this turnover rate tends to be much faster in view of the more rapid physiology in smaller organisms. Therefore, all cabazitaxel active metabolites were still measurable in the ritonavir-treated transgenic CYP3A mouse strain in contrast to the wild-type and *Abcb1a/1b*$^{-/-}$ mice, in which DM2 and docetaxel were not detectable anymore. As also observed previously (Loos, 2023), ritonavir had a clear impact on the active metabolite formation, whereas coadministration of elacridar does not seem to affect the metabolite formation. Interestingly, all three active metabolites appear to be substrates for Abcb1 based on their brain and SIC *in vivo* data, albeit to various extents. DM2 seems to be the most potent substrate for the efflux transporter, although this could in part also be related to the much higher plasma concentrations of this metabolite compared to DM1 and docetaxel.

5. Conclusion

In the present study, we showed that the relative tissue distribution of orally administered cabazitaxel boosted with ritonavir could be drastically enhanced for organs usually protected by ABCB1 activity by the addition of elacridar, without influencing the plasma pharmacokinetics. This could be beneficial for patients suffering from metastasis, especially in the brain, but also for patients who acquired chemotherapy resistance due to ABCB1 upregulation in the tumor cells. In the future, prostate cancer patients could therefore possibly be treated with an oral cabazitaxel formulation using coadministration of at least ritonavir and possibly also elacridar. The adoption of oral cabazitaxel could represent a significant advancement in patient care, offering a more patient-friendly alternative to traditional intravenous therapy. This shift also promises cost savings for healthcare institutions and reduced labor intensity. Nevertheless, more research will be needed to assess the safety and efficacy in patients of applying boosted oral cabazitaxel.

6. Funding sources

This research did not receive any specific grant from funding agencies in the public, commercial, or not-for-profit sectors.

CRediT authorship contribution statement

Nancy H.C. Loos: . **Margarida L.F. Martins:** Writing – review & editing, Investigation. **Daniëlle de Jong:** Writing – review & editing, Data curation. **Maria C. Lebre:** . **Matthijs Tibben:** Writing – review & editing, Supervision. **Jos H. Beijnen:** Writing – review & editing, Supervision. **Alfred H. Schinkel:** .

Declaration of competing interest

The research group of A.H. Schinkel receives revenue from commercial distribution of some of the mouse strains used in this study. Jos H. Beijnen is a part-time employee and (indirect) stockholder of Modra Pharmaceuticals, a spin-out company of The Netherlands Cancer Institute, developing oral taxane formulations. Jos H. Beijnen also holds (partly) a patent on oral taxane formulations. The other authors declare that they have no known competing financial interests or personal relationships that could have appeared to influence the work reported in this paper.

Data availability

Data will be made available on request.

Appendix A. Supplementary material

Supplementary data to this article can be found online at https://doi.org/10.1016/j.ijpharm.2023.123708.

References

Armstrong, C.M., Gao, A.C., 2015. Drug resistance in castration resistant prostate cancer: resistance mechanisms and emerging treatment strategies. Am. J. Clin. Exp. Urol. 3 (2), 64–76.

Bachmeier, C.J., et al., 2005. Quantitative assessment of HIV-1 protease inhibitor interactions with drug efflux transporters in the blood-brain barrier. Pharm. Res. 22 (8), 1259–1268.

Bao, X., et al., 2020. Protein Expression and Functional Relevance of Efflux and Uptake Drug Transporters at the Blood-Brain Barrier of Human Brain and Glioblastoma. Clin. Pharmacol. Ther. 107 (5), 1116–1127.

Bhambhvani, H.P., et al., *Prostate Cancer Brain Metastases: A Single-Institution Experience.* World Neurosurg, 2020. **138**: p. e445-e449.

Choudhuri, S., Klaassen, C.D., 2006. Structure, function, expression, genomic organization, and single nucleotide polymorphisms of human ABCB1 (MDR1), ABCC (MRP), and ABCG2 (BCRP) efflux transporters. Int. J. Toxicol. 25 (4), 231–259.

Darwich, A.S., et al., 2014. Meta-analysis of the turnover of intestinal epithelia in preclinical animal species and humans. Drug Metab. Dispos. 42 (12), 2016–2022.

de Bono, J.S., et al., 2010. Prednisone plus cabazitaxel or mitoxantrone for metastatic castration-resistant prostate cancer progressing after docetaxel treatment: a randomised open-label trial. Lancet 376 (9747), 1147–1154.

de Weger, V.A., et al., 2021. A Phase 1 Dose-Escalation Study of Low-Dose Metronomic Treatment With Novel Oral Paclitaxel Formulations in Combination With Ritonavir in Patients With Advanced Solid Tumors. Clin. Pharmacol. Drug Dev. 10 (6), 607–621.

EMA. *Assessment Report for Jevtana (cabazitaxel)*. 2011 [cited 2022 20-11-22]; 20 January 2011:[Available from: https://www.ema.europa.eu/en/documents/assessment-report/jevtana-epar-public-assessment-report_en.pdf.

FDA, U.S.F.a.D.A. *Prescribing information Jevtana (cabazitaxel)*. 2010 [cited 2022 15-11-2022]; 2010:[Available from: https://www.accessdata.fda.gov/drugsatfda_docs/label/2010/201023lbl.pdf.

Fracasso, P.M., et al., 2004. Phase I study of docetaxel in combination with the P-glycoprotein inhibitor, zosuquidar, in resistant malignancies. Clin. Cancer Res. 10 (21), 7220–7228.

Hammond, J., et al., 2022. Oral Nirmatrelvir for High-Risk, Nonhospitalized Adults with Covid-19. N. Engl. J. Med. 386 (15), 1397–1408.
Hendrikx, J.J., et al., 2013. P-glycoprotein and cytochrome P450 3A act together in restricting the oral bioavailability of paclitaxel. Int. J. Cancer 132 (10), 2439–2447.
Hendrikx, J.J., et al., 2014. Oral co-administration of elacridar and ritonavir enhances plasma levels of oral paclitaxel and docetaxel without affecting relative brain accumulation. Br. J. Cancer 110 (11), 2669–2676.
Holmstock, N., et al., 2010. In situ intestinal perfusion in knockout mice demonstrates inhibition of intestinal p-glycoprotein by ritonavir causing increased darunavir absorption. Drug Metab. Dispos. 38 (9), 1407–1410.
Ikezoe, T., et al., 2004. HIV-1 protease inhibitor, ritonavir: a potent inhibitor of CYP3A4, enhanced the anticancer effects of docetaxel in androgen-independent prostate cancer cells in vitro and in vivo. Cancer Res. 64 (20), 7426–7431.
Kharasch, E.D., et al., 2008. Mechanism of ritonavir changes in methadone pharmacokinetics and pharmacodynamics: II. Ritonavir effects on CYP3A and P-glycoprotein activities. Clin. Pharmacol. Ther. 84 (4), 506–512.
Kuppens, I.E., et al., 2007. A phase I, randomized, open-label, parallel-cohort, dose-finding study of elacridar (GF120918) and oral topotecan in cancer patients. Clin. Cancer Res. 13 (11), 3276–3285.
Li, W., et al., 2018. P-glycoprotein and breast cancer resistance protein restrict brigatinib brain accumulation and toxicity, and alongside CYP3A, limit its oral availability. Pharmacol. Res. 137, 47–55.
Li, W., et al., 2021. ABCB1 and ABCG2 Control Brain Accumulation and Intestinal Disposition of the Novel ROS1/TRK/ALK Inhibitor Repotrectinib, While OATP1A/1B, ABCG2, and CYP3A Limit Its Oral Availability. Pharmaceutics 13 (11).
Loos, N.H.C., et al., 2023. Enhancement of the Oral Availability of Cabazitaxel Using the Cytochrome P450 3A (CYP3A) Inhibitor Ritonavir in Mice. Mol. Pharm.
Macchiagodena, M., Pagliai, M., Procacci, P., 2021. Characterization of the non-covalent interaction between the PF-07321332 inhibitor and the SARS-CoV-2 main protease. J. Mol. Graph. Model. 110, 108042.
McBean, R., Tatkovic, A., Wong, D.C., 2021. Intracranial Metastasis from Prostate Cancer: Investigation, Incidence, and Imaging Findings in a Large Cohort of Australian Men. J. Clin. Imaging Sci. 11, 24.
Miller, D.S., 2014. ABC transporter regulation by signaling at the blood-brain barrier: relevance to pharmacology. Adv. Pharmacol. 71, 1–24.
Myint, Z.W., Qasrawi, A.H., 2021. Prostate Adenocarcinoma with Brain Metastasis: A Surveillance, Epidemiology, and End Results Database Analysis 2010–2015. Med. Sci. Monit. 27, e930064.
Robey, R.W., et al., 2018. Revisiting the role of ABC transporters in multidrug-resistant cancer. Nat. Rev. Cancer 18 (7), 452–464.
Rock, B.M., et al., 2014. Characterization of ritonavir-mediated inactivation of cytochrome P450 3A4. Mol. Pharmacol. 86 (6), 665–674.
Schinkel, A.H., Jonker, J.W., 2003. Mammalian drug efflux transporters of the ATP binding cassette (ABC) family: an overview. Adv. Drug Deliv. Rev. 55 (1), 3–29.
Seruga, B., Ocana, A., Tannock, I.F., 2011. Drug resistance in metastatic castration-resistant prostate cancer. Nat. Rev. Clin. Oncol. 8 (1), 12–23.
Szakács, G., et al., 2008. The role of ABC transporters in drug absorption, distribution, metabolism, excretion and toxicity (ADME-Tox). Drug Discov. Today 13 (9–10), 379–393.
Tang, S.C., et al., 2013. Impact of P-glycoprotein (ABCB1) and breast cancer resistance protein (ABCG2) gene dosage on plasma pharmacokinetics and brain accumulation of dasatinib, sorafenib, and sunitinib. J. Pharmacol. Exp. Ther. 346 (3), 486–494.
Tang, S.C., et al., 2015. P-glycoprotein, CYP3A, and Plasma Carboxylesterase Determine Brain Disposition and Oral Availability of the Novel Taxane Cabazitaxel (Jevtana) in Mice. Mol. Pharm. 12 (10), 3714–3723.
van Eijk, M., et al., 2019. Cytochrome P450 3A4, 3A5, and 2C8 expression in breast, prostate, lung, endometrial, and ovarian tumors: relevance for resistance to taxanes. Cancer Chemother. Pharmacol. 84 (3), 487–499.
van Waterschoot, R.A., et al., 2009. Absence of both cytochrome P450 3A and P-glycoprotein dramatically increases docetaxel oral bioavailability and risk of intestinal toxicity. Cancer Res. 69 (23), 8996–9002.
Vermunt, M.A.C., et al., 2021. Pharmacokinetics of docetaxel and ritonavir after oral administration of ModraDoc006/r in patients with prostate cancer versus patients with other advanced solid tumours. Cancer Chemother. Pharmacol. 87 (6), 855–869.
Vrignaud, P., et al., 2013. Preclinical antitumor activity of cabazitaxel, a semisynthetic taxane active in taxane-resistant tumors. Clin. Cancer Res. 19 (11), 2973–2983.
Ward, K.W., Azzarano, L.M., 2004. Preclinical pharmacokinetic properties of the P-glycoprotein inhibitor GF120918A (HCl salt of GF120918, 9,10-dihydro-5-methoxy-9-oxo-N-[4-[2-(1,2,3,4-tetrahydro-6,7-dimethoxy-2-isoquinolinyl)ethyl]phenyl]-4-acridine-carboxamide) in the mouse, rat, dog, and monkey. J. Pharmacol. Exp. Ther. 310 (2), 703–709.
Yared, J.A., Tkaczuk, K.H., 2012. Update on taxane development: new analogs and new formulations. Drug Des. Devel. Ther. 6, 371–384.
Zhou, S.F., 2008. Drugs behave as substrates, inhibitors and inducers of human cytochrome P450 3A4. Curr. Drug Metab. 9 (4), 310–322.
Zhu, Y., et al., 2013. Inhibition of ABCB1 expression overcomes acquired docetaxel resistance in prostate cancer. Mol. Cancer Ther. 12 (9), 1829–1836.